Springer

KSME

Journal of Mechanical Science and Technology 24 (8) (2010) 1623~1629
www.springerlink.com/content/1738-494x
DOI 10.1007/s12206-010-0527-9

Tooling device design for vibration-assisted high speed shaping of PMMA †

Md. Golam Mostofa[1], J. H. Noh[1], H. Y. Kim[2], J. H. Ahn[3] and D. B. Kang[3,*]

[1]*Intelligent Control and Automation Division, Department of Mechanical Engineering, Pusan National University, Busan, 609-735, Korea*
[2]*Research Institute of Mechanical Technology, Pusan National University, Busan, 609-735, Korea*
[3]*School of Mechanical Engineering, Pusan National University and ERC/NSDM, Busan, 609-735, Korea*

(Manuscript Received July 21, 2009; Revised December 31, 2009; Accepted May 30, 2010)

Abstract

PMMA optical components that are used as one of the most important parts of high precision equipments and machines are increasingly replacing the glass due to the various advantages of PMMA. Especially in Light Guide Panels, the PMMA sheet that is used in Liquid Crystal Displays plays an important role in scattering the incident light and requires very fine machining as the sheet is directly related to the optical characteristics of the panels. The High Speed End milling and High Speed Shaping processes that are widely adopted and applied to the precise machining of Light Incident Plane still have quality problems, such as cracks, breakages, poor waviness, and straightness. This paper presents the tooling device design for machining a Light Incident Plane through vibration-assisted High Speed Shaping for increasing the optical quality by minimizing the above-mentioned problems. The cutting tool and the tool post presented in this paper are designed by the authors to increase the magnitude of the cutting stroke by adopting the resonant frequency without weakening the stiffness and to reduce vibrations during even high speed feeding. The dynamic characteristics of the cutting tool and the tool post are evaluated through simulation and experiment as well. The results reveal very appropriate dynamic characteristics for vibration-assisted High Speed Shaping.

Keywords: High speed end milling; High speed shaping; Light guide panel; Resonance; Vibration cutting

1. Introduction

PMMA (Polymethyl-methacrylate) has been replacing the glass in the optics and display industry due to its lightness of weight, easy machinability, ease of material handling, and greater transparency (93%) with regard to light than glass (90%). Even in the Light Guide Panel (LGP) of a Back Light Unit (BLU), which uniformly scatters the incident light over the whole display area, one edge plane, which is called the Light Incident Plane (LIP) of a PMMA sheet, plays an important role in refracting the incident light. Given that light falls on LIP, the optical properties and the qualities of the LIP surface are very important. Therefore it is important to develop an appropriate machining process for getting a better LIP.

High Speed End milling (HSE) is widely used to generate a comparatively plain surface and to cut out four sides of a PMMA sheet for fitting it in the frame in which a gate that is generated during the production of the PMMA sheet is also removed. Along with HSE for some applications, High Speed Shaping (HSS) is applied for improving the optical characteristics and removing defects, such as waviness and edge breakage of the LIP that are caused by HSE operation. Besides HSS, there are other efficient cutting processes that use CO_2 lasers [1-4] or a Single Crystal Diamond (SCD) tool [5] for getting the ultra fine surfaces. It was shown that in laser cutting, the average surface roughness, Ra, was less than 1 μm and that the Heat Affected Zone (HAZ) ranged between 0.12 and 0.37 mm [2]. Under an SCD turning process, the value of the surface roughness was 20nm [5].

For the application of PMMA in LGPs, the HAZ will lower the light transmission inside the PMMA and the ultra fine surface will reduce the scattering of the light at the LIP. Basic investigations show that the application of HSS addresses the waviness and edge breakage but still leaves a problem with regard to the straightness of the LIP. The impact at the beginning of HSS, which causes vibrations at the tool plate and the clamping chuck as well, and the high depth-of-cut, which causes deviations of the PMMA sheet during machining and high friction between the cutting tool and the workpiece, are responsible for the lack of straightness of the LIP.

To overcome these problems, a new method of vibration-assisted HSS is adopted by combining vibration cutting with HSS. Further, a machine tool post is designed for the operation. Many studies have proved – not only theoretically but also experimentally - that a vibrational tool can greatly reduce

† This paper was recommended for publication in revised form by Associate Editor Dae-Eun Kim

* Corresponding author. Tel.: +82 51 510 3087, Fax.: +82 51 581 3087
E-mail address: dbkang@pusan.ac.kr

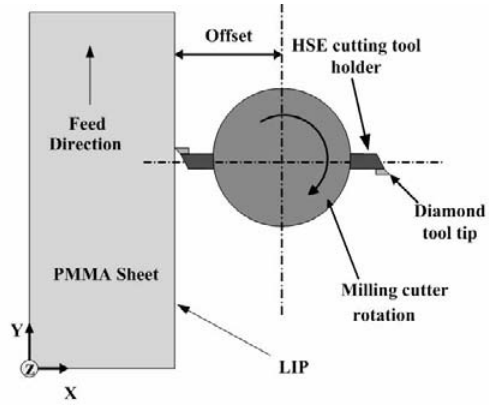

(a) HSE for the LIP

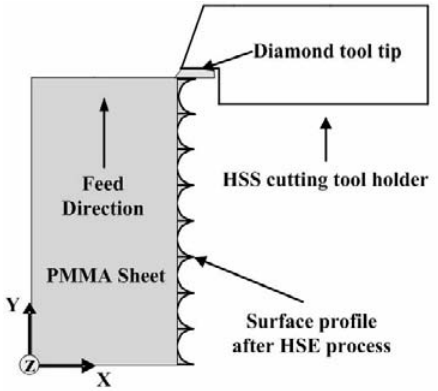

(b) HSS for the LIP

Fig. 1. HSE and HSS processes for the LIP.

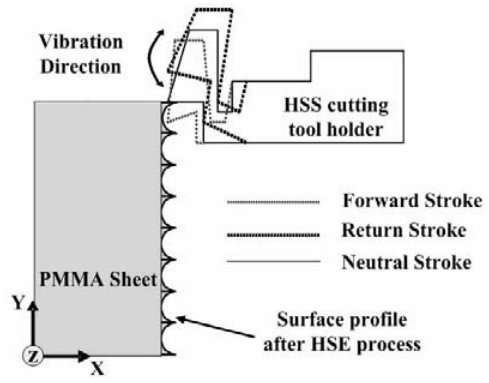

Fig. 2. Schematic of vibration-assisted HSS.

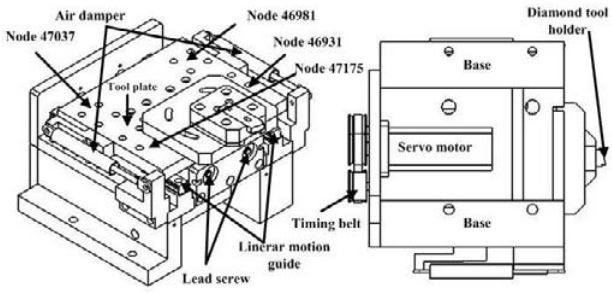

(a) Isometric View (b) Bottom View

Fig. 3. Structure of the tool post for HSS.

the cutting forces during cutting due to a considerable reduction of the friction between the workpiece and the cutting tool [6-12].

The objective of this research is to design a proper vibrational tooling device for vibration-assisted HSS based on the dynamic characteristics of a machine structure.

2. Machine structure for vibration-assisted HSS

2.1 Description of the machine structure

Fig. 1 shows the machining process for the LIP of a PMMA sheet; the process is composed of both HSE and HSS. The main purpose of the HSE process is to size the raw PMMA materials – following the injection molding process – to the BLU frame, wherein the tool holder of the HSE rotates at a very high speed of over 30,000 RPM. As the PMMA sheet is fed at a rather slow rate in comparison with the rotational speed, very fine diamond particles on the HSE tool holder can achieve a very small amount of Material Removal Rate (MRR) per tooth, which consequently result in a periodically waved profile similar to the serrations on the surface of the LIP. For better optical characteristics, the HSS process shown in Fig. 1(b) removes this spatial waviness in the direction of feeding and shapes very fine grooves on the LIP surface at a very high feedrate of up to 1.2 meters per second and at a very small depth-of-cut. Even though the HSS process improves the optical characteristics, the instant impact and large cutting forces due to the high feedrate cause breakage and/or lack of straightness.

Fig. 2 shows a schematic of vibration-assisted HSS for overcoming the limits of conventional HSS process. Through a micro actuator like PZT, the cutting tool vibrates at a frequency that escapes the natural frequencies of the machine structure. When the cutting tool vibrates, the PMMA sheet is fed in the forward direction and the material is removed repeatedly through sequential cutting. Thus, there is a relative motion between the workpiece and the cutting tool. The applied frequency of the cutting tool is very important with regard to vibrational cutting as it defines the maximum cutting speed that can be applied.

Fig. 3 shows the machine structure of a tool post for HSS. The tool post is composed of a base, tool plate, motor, timing belt, linear motion guide, and air dampers. The tool post is driven by a servo motor and two parallel lead-screws with a resolution of 1 um for adjusting the depth-of-cut of the diamond cutting tool in the x direction.

Compared to mechanical gears, the timing belt that combines the servo motor with dual lead screws can impart a damping effect and achieve low noise under even high speeds. To reduce the vibration that is caused by the impact force at the beginning of HSS, two air dampers are used with a reaction force of 30 N at the full-stroke compressed position.

Table 1. Conditions of the simulation.

1	Materials are made of structural steel.
2	Servo motor vibration is not considered.
3	All connections in assembly are considered to be fastening.
4	Timing belt model is not inserted in the simulation. (for different material).
5	Meshing is undertaken for individual parts.
6	A spring element is considered in linear motion guide. (Spring stiffness value is taken from the design manual).
7	Vibration due to bearings is ignored
8	The clamp boundary condition is applied to the base plate.
9	Excitation is given by the load

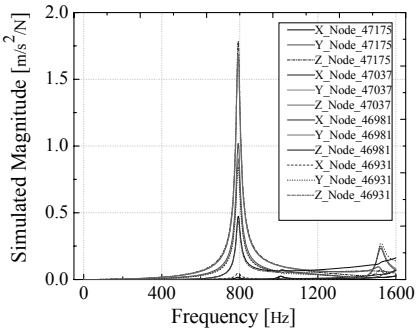

Fig. 4. Frequency response functions of the tool post – Simulation.

During the cutting process, a PMMA sheet is vacuum-chucked and the stage with the PMMA sheet is fed in the y direction at a very high speed by a linear motor that is adequate for high velocity and acceleration.

2.2 Design and dynamic analysis of the tool post

Dynamic characteristics are analyzed for identifying the stiffness and natural frequencies of the tool post system for designing the optimal parameters of the vibrational cutting tool. As a forced vibration will be applied by the micro actuator to the cutting tool, the cutting tool will vibrate as will the tool post. If the natural frequency of the tool post and the actuating frequency of the cutting tool coincide, then resonance will occur. When the vibration magnitude of the tool post at this resonant frequency becomes very large, the tool tip on the tool post will deviate from its desired direction of cutting to other directions. Therefore, it is very important to avoid the resonant frequency of the tool post for applying the frequency to the cutting tool. That is why the design of the tool post is critical for vibration-assisted HSS.

The tool post design and dynamic analysis have been conducted through CATIA V5 R15 in consideration of the damper structure. The conditions of simulation for harmonic dynamic analysis in the frequency domain are listed in Table 1.

2.3 Simulation results

Fig. 4 shows the Frequency Response Functions (FRFs) that

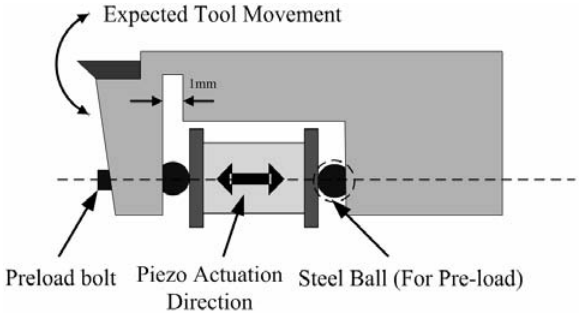

(a) Vibration cutting tool design and actuator setup

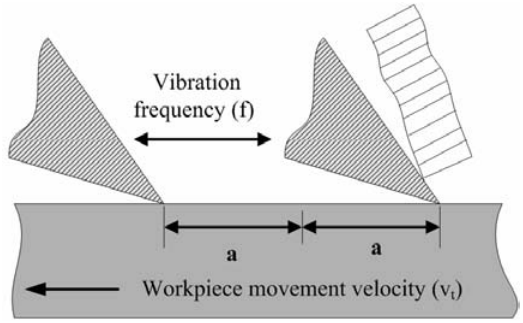

(b) Principle of vibration cutting

Fig. 5. Proposed mechanisms of vibration-assisted HSS.

are plotted from the simulation data. For all the selected nodes (see Fig. 3 for node positions) shown in Table 2, the magnitude is maximized at some particular frequencies, which indicates that those frequencies are the natural frequencies of the tool post. Four nodes are randomly selected on top of the tool plate.

The magnitude-vs.-frequency plot in the tri-axial directions shows that there are three natural frequencies of the tool post within the range of up to 1.6 kHz and that the first natural frequency is around 789Hz. This means the feeding structure with dual leadscrews is stiff enough [17-18] to minimize deflections even for large cutting forces or instant impacts.

3. Design of the vibration cutting tool for vibration-assisted HSS

3.1 Design of the vibration cutting tool

In order to realize better surface quality and better cutting performance in vibration-assisted HSS, the tool vibration technique that is based on PZT actuator is chosen. Fig. 5 (a) shows the design of the cutting tool for vibration-assisted HSS.

When the PZT actuator that is inserted in the extracted empty space of the cutting tool holder repeatedly expands and shrinks according to the control signals, deflections occurs in the vertical direction of the tool tip because the notch at the front of the cutting tool holder will act as a hinge point that is identical to the mechanism of a cantilever beam. Two steel balls are also inserted to ensure the point contacts between the PZT actuator and the cutting tool holder since the mismatch of the center-line along the direction of vibration causes signifi-

Table 2. Natural frequencies of the tool post for the selected nodes – Simulation.

Node No.	Frequency	X-Direction [Hz]	Y-direction [Hz]	Z-direction [Hz]
47175	1st	789	790	790
	2nd	1006	1014	1012
	3rd	1526	1520	1520
47037	1st	790	790	790
	2nd	1005	996	1009
	3rd	1509	1522	1508
46981	1st	792	790	790
	2nd	998	1014	1006
	3rd	1515	1520	1528
46931	1st	790	790	790
	2nd	1008	1000	1012
	3rd	1528	1522	1494

Table 3. Simulation results of modal analysis for the vibration cutting tool.

Mode	Frequency [Hz]
1	12220
2	13985
3	21035

cant and unexpected deflections of the tool tip. The preload bolt that is located at the front of the tool tip makes it possible to slightly adjust the resonant frequency for any mismatch in the resonant frequencies that arises from errors in the machining of cutting tool holder or the notch.

The cutting parameters that are related in vibration cutting are shown in Fig. 5 (b). Their relations are described as follows.

$$X = a\sin wt = a\sin 2\pi ft \tag{1}$$

$$V_t = 2\pi fa\cos(2\pi ft) \tag{2}$$

$$(V_t)_{\min} = 0 \tag{3}$$

$$(V_t)_{\max} = 2\pi fa \tag{4}$$

In the above, V_t is the cutting speed, a is the amplitude of the vibrational cutting tool, and f is the oscillating frequency. From the above equations, it is clear that the cutting speed, amplitude, and applied frequency are organically related to each other.

During cutting, if the applied cutting speed exceeds V_t, the cutting will transform from conventional HSS into vibration-assisted HSS. [7]

3.2 Dynamic analysis of the vibration cutting tool through Simulation

Zhang et al. [13] experimentally investigated that the increase of the vibrational amplitude of the tool in the UVC system improves the cutting quality and theoretically implemented by others [14-16]. However, the larger is the expansion distance of the PZT actuator, the smaller is the expansion force. That means that even under a notch mechanism, a large displacement cannot be achieved at high frequency due to the weak expansive force. Thus, the most effective way is to vibrate the cutting tool in the range of the resonant frequency.

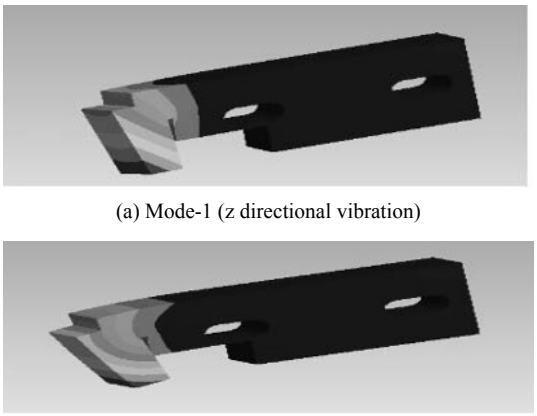

(a) Mode-1 (z directional vibration)

(b) Mode-2 (y directional vibration, cutting direction)

Fig. 6. Modes of the natural frequencies.

Fig. 6 shows the mode shapes of the cutting tool at its natural frequencies for the first and second modes obtained from ANSYS Workbench. The 2nd mode at around 13985 Hz in Fig. 6(b) is the mode where the cutting tool vibrates in the previously explained y direction, which is the desired direction of cutting.

The simulation results of the modal analysis for the vibrational cutting tool are listed in Table 3. Resonance will be present if the same frequency is applied in the cutting tool through PZT actuator as the natural frequency of the vibration cutting tool. Then, the tool tip deflection will be the sum of deflections that are caused by the PZT expansion force and the deflection through resonance, as two deflections are at the same phase of the frequency.

4. Experimental investigations

4.1 Measurement of the displacements of the tool tip

As mentioned in chapter 3.1, the cutting speed is related to both the tool tip deflection and the applied frequency. A basic investigation of tool tip deflections is necessary for finding out the critical cutting speed or the feedrate of the PMMA sheet at various applied frequencies. Fig. 7(a) shows a schematic diagram for investigations of the displacement of the designed vibration cutting tool. A PZT actuator, P-885.30, of Physik Instrumente is used for actuating the cutting tool with a high speed bipolar amplifier.

The tool tip deflections are measured through a laser displacement sensor with a resolution of 50 nm and sampling rates of up to 50 kHz.

From previous research [4-6, 17-18], it is known that tool tip deflections will be maximized at the natural frequency of the cutting tool. Thus, the applied voltages are fixed at 10, 20,

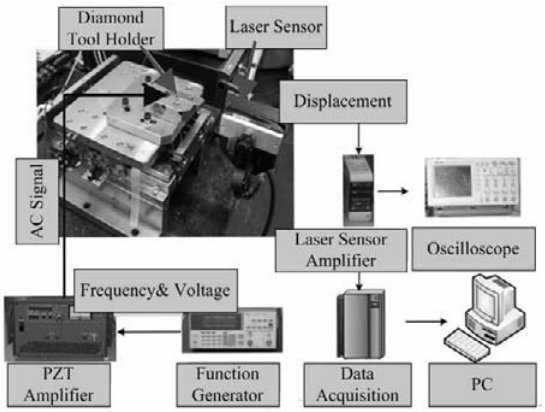

(a) Schematic diagram of displacement measurement for a diamond tool tip

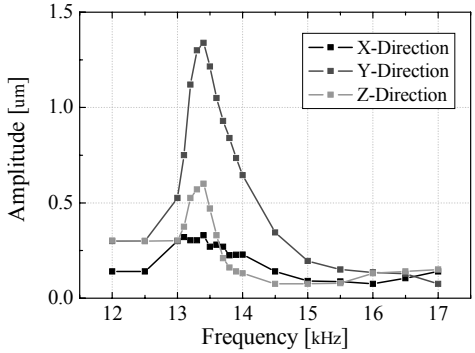

(b) Tool tip displacements for 10 V input

Fig. 7. Experimental setup and results for measurement of tool tip displacement.

and 30 Volts and the applied frequencies are varied from 12 kHz to 17 kHz for identifying the optimized oscillating frequency with a maximum displacement.

Experimental results are shown in Fig. 7(b) for input signals of 10 V. According to the simulation results, the amplitude should be only in the y direction at the second modal frequency but experimental results show that deflections are also found in the x and z directions. The investigation shows that the reason for these x- and z- directional deflections arises from the preload bolt of PZT, the eccentricity of the PZT load, and inevitable manufacturing and assembly errors. The cutting speeds shown in Table 4 are calculated from Eq. 5.

Experimental results show that the theoretically investigated harmony is negligible in comparison with the simulated harmony of 4.2 % at the applied frequency and that the use of the natural frequency is advantageous for increasing the tool tip deflection, as explained previously.

The dynamic characteristics are identified through an impact hammer modal test for the designed tool post. Fig. 8(a) shows the experimental setup of the impact hammer modal test where the accelerometer, B&K Triaxial Charge Accelerometer of Type 4326A that covers a range of up to1.6 kHz, is attached to the tool plate of the tool post.

The experimental Frequency Response Functions (FRFs)

Table 4. Optimized parameters for vibration-assisted HSS.

Applied volt [V]	10	20	30
Simulation Frequency [kHz]	13.98	13.98	13.98
Experimental Frequency [kHz]	13.4	13.4	13.4
Error in Frequency [%]	4.18	4.18	4.18
Amplitude (x-direction)	0.4	0.53	0.9
Amplitude (y-direction)	1.34	2	2.75
Amplitude (z-direction)	0.6	0.85	1.75
Cutting Speed (mm/s, calculated for the amplitude in the y direction)	122	168	230

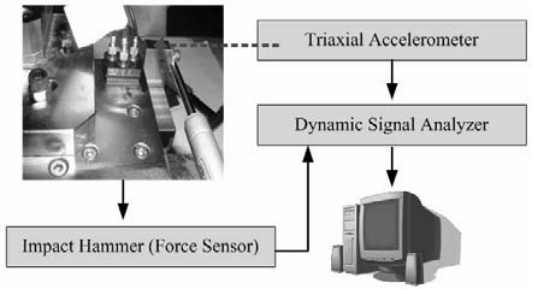

(a) Experimental setup for FRF measurements of the tool post

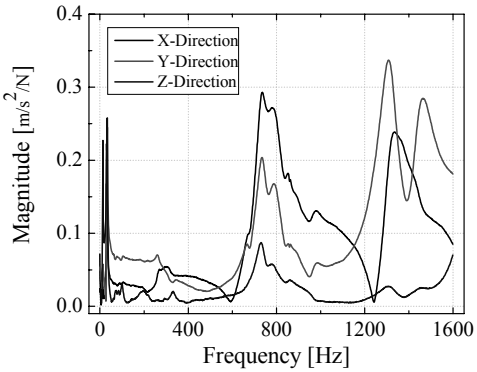

(b) Experimental FRFs of the tool post from the impact hammer modal test

Fig. 8. Impact hammer modal test for the tool post.

are shown in Fig. 8(b) for the three axes. The axis with the maximum magnitude is the x direction, which is the direction for depth-of-cut control and the weakest direction of the tool post. The plot is limited up to 1.6 kHz because of the testing instrument's limitation.

4.2 Dynamic identification of the tool post

Fig. 9 shows a comparison of the simulated and experimental FRFs. The first natural frequency from simulation is found to be around 789 Hz and the experimental frequency is around 736 Hz; hence, the percentage difference is only 6.7 %, which may be caused due to some conditions that are ignored, such as mass and other aspects between the original tool post and the modeled tool post. The first natural frequency of the tool post is very high, which means the tool post has enough stiffness [17-19] to support the impact force even under conditions of high velocity and acceleration at the beginning of HSS.

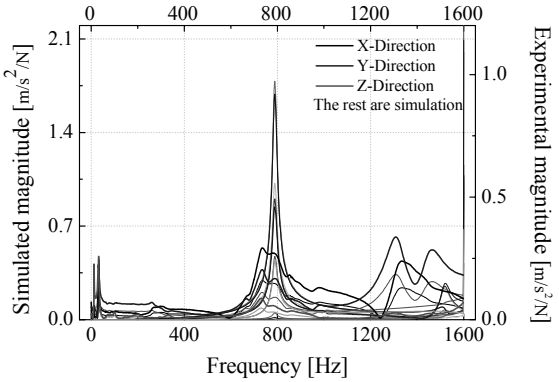

Fig. 9. Comparison of the simulated and experimental frequency responses.

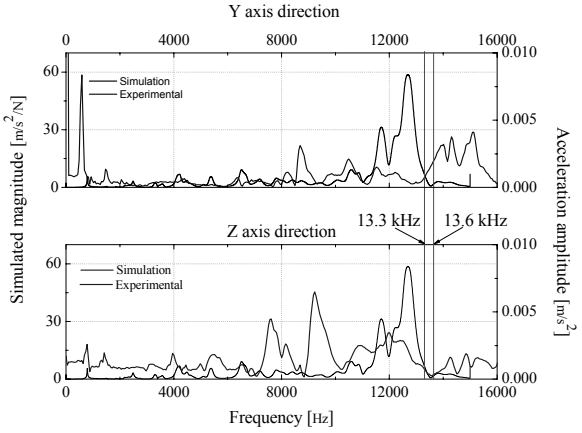

Fig. 10. Experimental frequency responses of the tool post up to 15 kHz.

4.3 Identification of the applied frequency for vibration-assisted HSS

In the previous subsection, the FRFs of the tool post have been compared with the experimental FRFs up to 1.6 kHz. However, as the applied frequency for the cutting tool is around 13.4 kHz, FRFs over 1.6 kHz and up to even 15 kHz should be identified. However, an experimental method that uses an impact hammer or shaker is not adequate due to its dynamic limitations. Thus, the dynamic characteristics of the tool post up to 15 kHz are verified through a simulated harmonic test and the results are compared with the frequency response results that are measured by the accelerometer.

Fig. 10 shows the FRFs of the tool post that are calculated from simulation data along the left y-axis and the frequency response curves that are experimentally measured from accelerometer data along the right y-axis. The figure reveals similar types of peaks and valleys for amplitudes. As the two vertical axes have different dimensions, an exact comparison is meaningless because the absolute magnitude cannot be gained without the known impact force. Nevertheless, the frequency where there is resonance can be identified.

Form both the simulated and experimental results, it is clear that the applied frequency of 13.4 kHz is surely well adopted within the range of no resonance, not only in the z direction but also in the y direction.

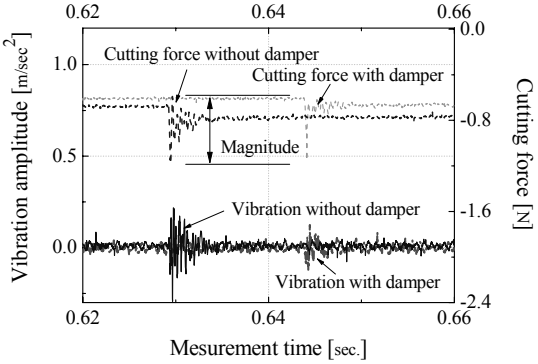

Fig. 11. Tool plate vibrations with/without the air damper.

4.4 Evaluation of the air damper

During the HSS process, the fast feeding with high acceleration causes the great impact between the tool post and the PMMA sheet. If vibrations due to the instant impact are not attenuated immediately, the surface quality cannot be guaranteed. In particular, the vibration-assisted HSS continuously vibrates the tool post and the machining tool during cutting; the resulting impact will cause more serious quality problems. To increase the damping effect at the beginning of cutting, including vibration-assisted HSS, two air dampers are attached between the tool plate and the base. Further, some cutting tests are conducted for the evaluation of air dampers in real cutting.

Fig. 11 shows a comparison of the cutting forces and vibrations that occur during the cutting process. The cutting speed is set at 100 mm/s and the other conditions are same for two cases.

Vibrations that are created at the tool plate are lower and diminish immediately for the tool post with air dampers even under almost the same amount of force, when the feed rate is kept constant.

5. Conclusions

In this paper, a cutting tool and a tool post for the vibration-assisted high speed shaping (HSS) of PMMA sheet are designed and the dynamics characteristics are identified through not only simulation but experiment. The shape of the cutting tool is optimized enough so that the tool resonates at the desired natural frequency and avoids some resonant frequency modes of the tool post. The conclusions are as follows.

(1) The use of the resonant mode can increase the displacement of the cutting tool tip without weakening the stiffness of the cutting tool holder for increasing the deflection.

(2) The dynamic characteristics of the tool post, as identified through simulation, match well with the experimental characteristics. And the applied frequency is selected in the stable range.

(3) The stiffness of the tool plate is increased and damping effects are significantly improved by the addition of air dampers at either side of the tool plate.

References

[1] J. P. Davim, C. Oliveira, N. Barricas and M. Conceição, Evaluation of cutting quality of PMMA Using CO_2 laser, *International Journal of advanced manufacturing technology*, 35 (9-10) (2008) 875-879.

[2] B. H. Zhou and S.M. Mahdavian, Experimental and theoretical analyses of cutting nonmetallic materials by low power CO2-laser, *Journal of Materials Processing Technology*, 146 (2004)188-192.

[3] J. P. Davim, N. Barricas, M. Conceição and C. Oliveira, Some experimental studies on CO2 laser cutting quality of polymeric materials, *Journal of Materials Processing Technology*, 198 (2008) 99-104.

[4] S. Morihiko, Y. Heiji, S. Kondo, M. Kawada and H. Akira, Experimental Investigation of Surface Roughness in Ultra-Precision Cutting of Plastics, *Journal of the Japan Society for Precision Engineering*, 67 (2) (2001)311-315.

[5] C. Nath and M. Rahman, Evaluation of Ultrasonic Vibration Cutting while machining Inconel 718, *International Journal of Precision Engineering and Manufacturing*, 9 (2) (2008) 63-68.

[6] D.E. Brehl, T.A. Dow, Review of vibration-assisted machining, *Precision Engineering*, 32 (2008) (153-172).

[7] C. Nath and M. Rahman, Effect of machining parameters in ultrasonic vibration cutting, *International Journal of Machine Tools and Manufacture*, 48 (2008) 965-974.

[8] M. Xiao, S. Karube, T. Soutome and K. Sato, Analysis of chatter suppression in vibration cutting , *International Journal Machine tools and manufacture*, 42 (2002) 1677- 1685.

[9] J. Kumabe, et al., Ultrasonic superposition vibration cutting of ceramics, *Precision Engineering*, 11 (2), (1989) 71-77.

[10] J. Kumabe and M. Hachisuka, Super-precision cylindrical machining, *Precision Engineering*, 6 (2) (1984) 67-72.

[11] A. V. Mitrofanov, N. Ahmed, V. I. Babitsky and V. V. Silberschmidt, Effect of lubrication and cutting parameters on ultrasonically assisted turning of Inconel 718, *Journal of Material Processing Technology*, 162-163 (2005) 649-654.

[12] J.-D. Kim and I.-H. Choi, Micro surface phenomenon of ductile cutting in the ultrasonic of optical plastics, *Journal of Material Processing Technology*, 68 (1997) 89-98.

[13] Y.-L. Zhang, Z.-M. Zhou and Z.-H. Xia, Diamond turning of titanium alloy by applying ultrasonic vibration, *Transactions of the Nonferrous Metals Society of China*, 15 (Special 3) (2005) 279-282.

[14] J. D. Kim and I. H. Choi, Characteristics of chip generation by ultrasonic vibration cutting with extremely low cutting velocity, *The International Journal of Advanced Manufacturing Technology*, 14 (1998) 2-6.

[15] V. I. Babitsky, A. N. Kalashnikov, A. Meadows and A.A.H.P. Wijesundara, Ultrasonically assisted turning of aviation materials, *Journal of Material Processing Technology*, 132 (2003) 157-167.

[16] M. Jin and M. Murakawa, Development of a particle ultrasonic vibration cutting tool system, *Journal of Material Processing Technology*, 68 (2001) 342-347.

[17] G. P. Zhang, Y. M. Huang, W. H. Shi and W. P. Fu, Predicting dynamic behaviors of a whole machining tool structure based on computer-aided engineering, *International Journal of Machine Tools & Manufacturing*, 42 (2003) 699-706.

[18] S. H. Jang and S. M. Kim, S. G. Kim, Y. H. Choi and J. K. Park, Structure Design Optimization of a Micro Milling Machine for Minimum Weight and Compliances Using Genetic Algorithm, *Proceedings of the 3rd International Workshop on Microfactory Technology*, August (2007) 23-24.

[19] Y.-S. Yi, Y. Y. Kim, J. S. Choi, J. h. Yoo, D. J. Lee, S. W. Lee and S. J. Lee, Dynamic analysis of a linear motion guide having rolling elements for precision positioning devices, *Journal of Mechanical Science and Technology*, 22 (2008) 50-60.

Golam Mostofa received his Bachelor degree in Mechanical Engineering from Bangladesh University of Engineering and Technology (BUET) in 2007. At present, he is pursuing his MS at Pusan National University (PNU). His research interests include industrial automation, system monitoring, computer-aided design and analysis, and optimizing mechanical system for best performance.

Dong Bae Kang received his B.S and M.S degrees in Mechanical Engineering from Pusan National University, Korea in 2001 and 2003. At present, he is pursuing his Ph.D course in Pusan National University. His research interests include industrial automation, status monitoring, system integration and precision machining.